14th IEA Heat Pump Conference
15-18 May 2023, Chicago, Illinois

High Efficiency Heat Pump Industrial Drying with Water Vapor-Selective Membranes

Andrew J. Fix, James E. Braun, David M. Warsinger*

Purdue University, School of Mechanical Engineering & Herrick Laboratories, 585 Purdue Mall, West Lafayette, IN 47907

Abstract

Convective drying processes consume a significant amount of energy within the industrial sector. Heat pump-based drying processes are gaining attention as a potential technology for enabling efficient, electricity-driven drying for various applications. In this work, we propose a new heat pump drying system concept that employs water vapor-selective membranes for active control of the air humidity in drying processes, termed the MemDry system. We developed system-level models for the MemDry and representative baseline systems based on the first and second laws of thermodynamics to explore energy trends and limitations of the concept. It was found that energy savings on the order of 30-40% are possible when high temperature, low humidity conditions are required for the drying process. Furthermore, membrane dehumidification could theoretically reduce required drying temperatures by 10-20℃ while still saving energy. The unique design of the MemDry system and its use of exhaust air condensation may improve heat pump COPs by as much as 2x. This theoretical work shows that the MemDry concept has significant potential to provide efficient, feasible, and controllable conditions for industrial heat pump drying applications.

Keywords: selective membranes; dehumidification; drying; Carnot; high temperature; thermodynamics; heat pump

1. Introduction and Background

1.1. Convective Drying Technologies

It has been estimated that thermal dehydration technologies account for anywhere between 10-20% of industrial energy consumption in developed countries [1]. Convective drying is one of the most common types of drying technologies, employed in drying food, pharmaceuticals, fabrics, chemicals, and more. Another common application for convective drying is residential clothes dryers, which constitute 3% of residential energy consumption [2]. Currently, industrial drying processes rely heavily on the combustion of fossil fuels [3]. More recently, there has been increased interest in moving away from combustion-based drying technologies, in favor of heat pump drying technologies [4].

Many different configurations and combinations of heat pump drying technologies have been proposed, including air-source [5], ground-source [6], solar assisted [7], chemical heat pumps [8], various forms of energy recovery, and more [4]. However, in their simplest form, the two categories of heat pump dryers are closed and open systems. Open dryers pull in ambient air, heat it up, send it to the drying process, and then simply exhaust the warm and humid air that leaves the drying process. In a closed heat pump dryer, instead of exhausting the warm and humid air leaving the drying process, it is instead passed through the vapor compression cycle's evaporator to condense water out of the air and is then reheated and recirculated [9].

Open heat pump systems can achieve high efficiency performance if the ambient conditions are very low humidity, but otherwise may be limited by the ambient conditions [3]. On the other hand, closed systems are not as dependent on the ambient conditions but must spend a considerable amount of energy condensing water

* Corresponding author. Tel.: +1-240-205-0440. *E-mail address:* dwarsing@purdue.edu.

out of the air. Conventional air conditioning technologies experience similar energy penalties when dealing with humidity [10]. Generally, closed heat pump dryers are more common in the literature, but even open systems could benefit from pre-dehumidification technologies. Thus, there is a need to identify innovative solutions to address the energy demands associated with air dehumidification in heat pump drying processes.

1.2. Water Vapor-Selective Membranes for Air Dehumidification

Recently, water vapor-selective membranes have gained interest in air conditioning research [11]. Conventional air conditioning technologies rely on cooling the air below its dew point to induce condensation dehumidification, and condensing water vapor requires a significant amount of energy [12]. Instead of relying on energy-intense phase-change dehumidification, selective membranes can mechanically separate water vapor out of air, which can save energy input depending on the system design [12], [13].

Most membranes used for air dehumidification are referred to as "dense" membranes [14]. For dehumidification membranes, a dense (non-porous) hygroscopic material, usually a polymer, is coated onto a support material. Because this hygroscopic layer is non-porous, air cannot easily penetrate, though the hygroscopic nature of the layer enables water vapor to transport across via the solution-diffusion process [15]. Some high-performance membrane materials for dehumidification include Pebax 1657 combined with graphene oxide [16], polyvinyl alcohol combined with triethylene glycol [17], and cellulose [19].

The two important performance metrics for the membrane materials are the permeance to water vapor and the air selectivity. The water vapor permeance simply describes the membrane's ability to pass water vapor. The air selectivity describes how well the membrane blocks air transport and is generally taken as the ratio of the water vapor permeance to the air permeance. Optimal membranes achieve both high selectivity and water vapor permeance. Top performing membranes generally achieve water vapor permeance on the order of 1,000-5,000 GPU, and selectivity up to 10,000 [16], [17]. However, the analysis in this work will provide high-level thermodynamic insight into the application of membrane dehumidification in industrial drying applications in a manner that does not rely on knowing or assuming values for these membrane material properties.

1.3. Scope and Novelty

While thermodynamic modeling for vacuum membrane dehumidification has been carried out extensively for air conditioning applications [13], [20]–[22], little-to-no work has been done in the field of industrial heat pump drying. This work, to the best of our knowledge, is the first to propose a hybrid membrane dehumidification and heat pump system configuration for efficient industrial drying applications. This analysis provides an introduction to the concept and explores the potential energy benefits through high-level, thermodynamic models that employ both theoretical and practical assumptions. The results provided in this paper will serve as a basis for further detailed modeling and prototyping efforts and can help establish a new sub-field within the heat pump and membrane research communities.

2. System Descriptions

2.1. Membrane Dehumidifier and Heat Pump Dryer System Description

In this work, we will refer to the system that combines membrane dehumidification and heat pump drying as the "MemDry" system. The left half of Figure 1 depicts the flow schematic of the MemDry system. Starting at State 1, relatively warm, saturated (100% relative humidity) air leaves the drying process and enters the dehumidification membrane module. A water vapor compressor maintains a low water vapor partial pressure on the top (permeate) side of the membrane at State 7 [23]. This difference in water vapor partial pressure draws humidity out of the drying process exhaust air while requiring no heat transfer. Then, the dry air at State 2 is reheated before being sent back to the drying process. The humidity that was removed between State 1 and State 2, is then slightly pressurized by the water vapor compressor to the second membrane module at State 8 and rejected across a membrane to the ambient air at State 4 [24].

The humid air at State 5 then passes through the evaporator of the vapor compression cycle, where heat is absorbed for reheating the process air (States 2 to 3). Condensing water vapor in this exhaust air is beneficial, as a significant portion of the heat transfer will come from the latent heat of vaporization. This means that, under certain conditions, warmer evaporator temperatures can be used, resulting in higher heat pump COPs. Plus, heat pump capacity requirements are lower, meaning smaller heat pump systems can be implemented.

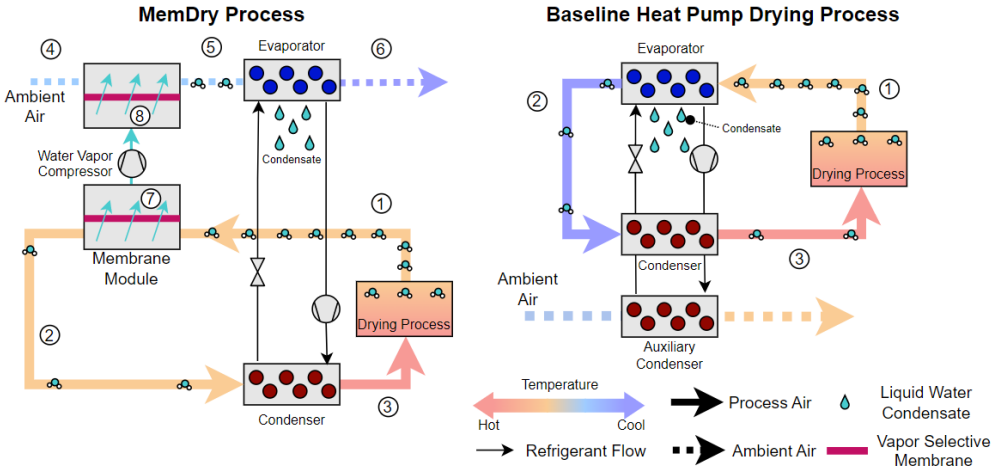

Figure 1. System schematics. (left) Membrane dehumidifier and heat pump dryer system schematic, referred to herein as the MemDry system. (right) Baseline, closed heat pump drying process.

2.2. Baseline Heat Pump Dryer System Description

In the baseline closed heat pump dryer system, shown in Figure 1 (right), State 1 and State 3 are identical to those states in the MemDry system. However, the relatively warm and humid air at State 1 is cooled to a lower temperature to induce condensation dehumidification. In this work, we model both systems such that the absolute humidity at State 2 is equivalent between both systems. But, because the air was cooled to induce condensation dehumidification, a significant amount of reheating must be provided by the condenser. While the condensation will provide a significant source of heat transfer in the baseline system as well, it is not strictly beneficial (as it is in the MemDry system) since it induces significant reheating requirements and lower evaporator temperatures are needed to maintain the desired humidity levels. Additionally, the condenser rate of heat transfer will be higher than the evaporator, so in order to maintain an energy balance within the drying process flow, an auxiliary condenser would be included to reject excess heat to an ambient air stream [2]. Figure 2 provides a sample psychrometric plot of the thermodynamic states in the two drying systems.

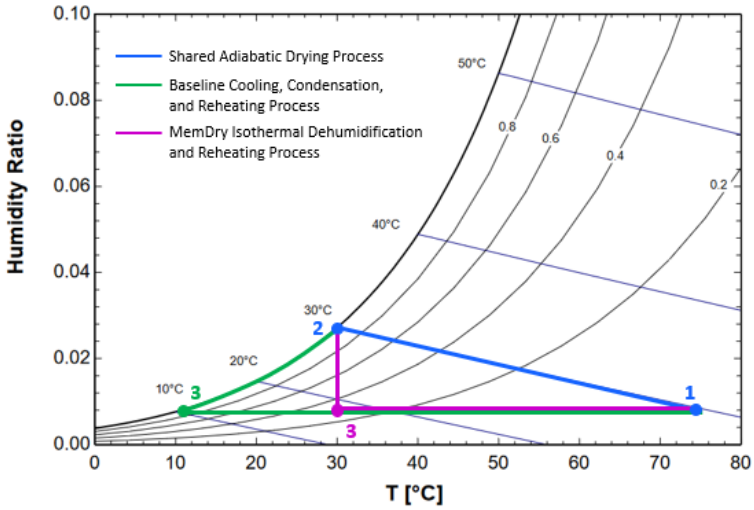

Figure 2. Sample psychrometric process plot showing the thermodynamic states within the drying cycle specific to the baseline system (green), MemDry system (pink), and shared isenthalpic drying process (blue). The supply temperature is shown as 75°C as an example.

3. Modeling Methodology

3.1. Modeling Overview

The models developed in this work are system-level, steady-state thermodynamic models based on a first-law analysis. Specific components are not modeled in detail (e.g., membrane area, heat exchanger area, membrane properties are not included in the model). This will become clear as the model is derived in the following sections. The models were developed in Engineering Equation Solver (EES), which is an iterative

solving software with built-in thermodynamic property functions for many fluids, including humid air [25]. Furthermore, some portions of the model were first replicated from prior published drying technology models before extending the framework to the MemDry system to ensure reasonable assumptions for the model. Overall, the intent of these theoretical models is to capture performance trends for the systems with both highly idealized assumptions and more practical assumptions and to assess key benefits and limitations.

3.2. Convective Drying Process Model and Validity

The convective drying process is modeled the same way for both systems in this work and is assumed to be a relatively ideal drying process. The supply temperature, T_3, and supply dew point temperature, $T_{\mathrm{DP},3}$, are set as inputs for most of the analyses. The supply dew point temperature is used as the metric for setting the dryer inlet humidity condition for convenience, as this will be directly tied to the evaporator temperature in the baseline system shown later. Thus, the inlet conditions, including the inlet humid air enthalpy, h_3, are known. To determine the dryer outlet conditions, we assume an ideal dryer where the drying occurs adiabatically (constant enthalpy) and the air leaving the drying process reaches 100% relative humidity [2]. These two critical assumptions are given by Equations 1 and 2.

$$h_1 = h_3 \tag{1}$$

$$RH_1 = 100\% \tag{2}$$

Thus, the inlet and outlet humid air conditions are known. In this work, a specific drying process is not explicitly modeled (conveyer drying, batch drying, etc.) Furthermore, we do not consider any dynamic behavior associated with the type of material being dried, thermal mass, or the change in drying rate as the water content changes in the product material. Similar simplifications have been made in other works and are justified here since the focus is on providing a comparative analysis between two heat pump technologies meeting the same theoretical drying load. Models from prior published work [2] were obtained for comparing inlet and outlet temperature conditions for different scenarios. It was found that the maximum error between our model and the prior model's temperature calculations was less than 1%, giving confidence that our drying process model was consistent with other works.

3.3. Vapor Compression Cycle Model

Both the MemDry and baseline systems incorporate a heat pump for process air heating. Due to the high temperature lift in this application (up to 130℃ in some cases), a more complex cycle architecture would be needed to achieve competitive COPs. However, this work focuses more on the comparison of the MemDry system to the baseline system, emphasizing the benefits of membrane dehumidification. So, to simplify the modeling of the vapor compression cycle energy requirements, two sets of results are presented. One set of results looks at the most ideal scenario and applies Carnot COPs to evaluate energy input requirements for the heat pumps. The Carnot cooling COP and heating COP, based on the thermodynamic states in the baseline system, are given by Equations 3 and 4, respectively.

$$COP_{Carnot,C} = \frac{T_2}{T_3 - T_2} \tag{3}$$

$$COP_{Carnot,H} = \frac{T_3}{T_3 - T_2} \tag{4}$$

Similar equations can be applied to the MemDry system but replacing T_2 with T_6. The second set of results that are presented apply a second law efficiency (η_{II}) to estimate real vapor compression cycle COPs for high temperature lift applications. Based on a review of detailed modeling efforts for high-temperature heat pumps employing two stage compression with some form of economization, it was found that the second law efficiency was around 0.40 across a broad range of conditions [26], [27]. The "practical" results in this work apply this second law efficiency to the Carnot COP to estimate "real" COPs, shown in Equation 5.

$$COP = COP_{Carnot} * \eta_{II} \tag{5}$$

Thus, the vapor compression cycle performance can be reasonably captured using the straightforward framework to compare the two systems and assess the benefits of adding membrane dehumidification.

3.4. Baseline Heat Pump Dryer System Model

Since the drying process is modeled identically in both systems, the remaining model derivations will focus on the portions of the two systems that remove humidity from the process air and reheat the process air.

3.4.1. Evaporator Energy Balance

The primary purpose of the evaporator in the baseline system is to provide dehumidification to the process air before it is reheated and sent back into the drying process. The temperature of the air at State 2 is used as an input or is varied in some of the following analyses. Since the air at State 1 is 100% relative humidity, State 2 will also be 100% relative humidity. The air-side energy balance on the evaporator in the baseline system is then given by Equation 6.

$$\dot{Q}_{evap,b} = \dot{m}_a(h_1 - h_2 - (\omega_1 - \omega_2)h_w) \tag{6}$$

Here, $\dot{m}_\mathrm{a}$ is the mass flowrate of air (on a dry basis) in the drying cycle, h represents the enthalpy of humid air, ω is the air humidity ratio, and h_w is the enthalpy of liquid water. In a steady state vapor compression cycle, the evaporator heat transfer rate is always less than the condenser heat transfer rate. So, we know that if the latent load is met by the evaporator, we will have sufficient (actually excess) heat available to reheat the process air in the condenser. Thus, the power consumption for the baseline heat pump system is based on the evaporator load, given by Equation 7 [28].

$$\dot{W}_b = \frac{\dot{Q}_{evap,b}}{COP_c} \tag{7}$$

Here, COP_c is the cooling coefficient of performance and can either be the Carnot COP ($\eta_\mathrm{II} = 1$) or practical COP ($\eta_\mathrm{II} = 0.4$), depending on the result being presented.

3.4.2. Condenser Energy Balance

Based on an energy balance for a vapor compression cycle, we can calculate the heat transfer rate in the condenser ($\dot{Q}_\mathrm{cond,b}$) according to Equation 8.

$$\dot{Q}_{cond,b} = \dot{W}_b + \dot{Q}_{evap,b} \tag{8}$$

The actual heat transfer rate required for reheating the process air ($\dot{Q}_\mathrm{heat,b}$) from State 2 to State 3 is given by Equation 9.

$$\dot{Q}_{heat,b} = \dot{m}_a(h_3 - h_2) \tag{9}$$

The enthalpy at State 2 (h_2) is known based on the set temperature and knowing the relative humidity is 100%, and the enthalpy at State 3 (h_3) is known based on the set drying temperature (T_3) and knowing that $\omega_3 = \omega_2$. As discussed before, excess heat is available on the condenser side of the vapor compression cycle due to the energy balance, therefore, the heat transfer rate in the auxiliary condenser is given by Equation 10.

$$\dot{Q}_{aux} = \dot{Q}_{cond,b} - \dot{Q}_{heat,b} \tag{10}$$

3.5. MemDry System Model

For the MemDry system, the vapor compression cycle is implemented slightly differently, requiring different energy balances, and the membrane dehumidification portion of the system model must be presented.

3.5.1. Membrane Dehumidification Governing Equations

Air leaving the drying process at State 1 enters the membrane module. In order to fairly compare both systems in this analysis, the dew point temperature at State 2 ($T_\mathrm{DP,2}$) is equivalent in both systems for all analyses. This dew point temperature has an associated humidity ratio (ω_2) and water vapor partial pressure

($P_{v,2}$). Thus, $P_{v,2}$ is known/set in the model. The low vacuum vapor pressure ($P_{v,7}$) required to meet this dehumidification load is set based on a given pinch point vapor pressure difference ($\Delta P_{v,pinch}$). Thus, $P_{v,7}$ can be calculated according to Equation 11.

$$P_{v,7} = P_{v,2} - \Delta P_{v,pinch} \tag{11}$$

Estimating vacuum vapor pressure in this manner is analogous to estimating vapor compression cycle evaporator or condenser temperatures based on assumed pinch point temperature differences. In this work, we use a pinch vapor pressure difference of 0.5 kPa for the practical scenarios, falling in the range analyzed by [21], and 0 kPa for the ideal scenarios, representing a mass exchanger with 100% effectiveness. State 7 and State 8 are both assumed to be pure water vapor, which implies that the membranes are perfectly selective. This assumption has been applied in many modeling works for assessing theoretical thermodynamic energy requirements of the technology [20], [21]. The mass flowrate of water vapor removed in the dehumidification process is given by Equation 12.

$$\dot{m}_v = \dot{m}_a(\omega_1 - \omega_2) \tag{12}$$

Next, we assume that when the water vapor is rejected to the exhaust air, the relative humidity is brought to 90% at State 5. With this assumption, a mass balance can determine the exhaust air flowrate ($\dot{m}_{a,ex}$) needed to achieve this condition.

$$RH_5 = 90\% \tag{13}$$

$$\dot{m}_v = \dot{m}_{a,ex}(\omega_5 - \omega_4) \tag{14}$$

Now, knowing the water vapor partial pressure at State 5, the rejection side water vapor partial pressure, $P_{v,8}$, can be calculated using the same pinch point vapor pressure difference as before.

$$P_{v,8} = P_{v,5} + \Delta P_{v,pinch} \tag{15}$$

The power consumption of the water vapor compressor is calculated by assuming an isentropic efficiency, as shown in Equation 16 [22], [28].

$$\dot{W}_{WVC} = \dot{m}_v \frac{h_{v,8s} - h_{v,7}}{\eta_{WVC}} \tag{16}$$

Here, $h_{v,7}$ is the enthalpy of water vapor at a pressure of $P_{v,7}$ and a temperature of T_1. $h_{v,8s}$ is the enthalpy of the water vapor at a pressure of $P_{v,8}$ under isentropic compression from State 7. η_{WVC} is the compressor isentropic efficiency, taken as 1 for the ideal scenarios and 0.7 for the practical scenarios [22].

3.5.2. Condenser Governing Equations

The membrane dehumidification process is assumed to be isothermal ($T_2 = T_1$). Therefore, the condenser energy balance is simply given by Equation 17.

$$\dot{Q}_{cond,M} = \dot{m}_a(h_3 - h_2) \tag{17}$$

It should be noted that, in the baseline system, the evaporator was the minimum load that must be met in the system, and we know that as long as the evaporator load is met, there will be sufficient heat for reheating in the condenser. However, in the MemDry system, the reheating load in the condenser is the minimum load that must be met, and the evaporator load does not affect the drying process (other than the evaporator temperature affecting the heat pump COP). Thus, the energy input for reheating the process air is given by Equation 18 and is based on the condenser load.

$$\dot{W}_{cond,M} = \frac{\dot{Q}_{cond,M}}{COP_H} \tag{18}$$

Here, COP_H is the heating coefficient of performance and can either be the Carnot COP or practical COP (depending on the result being presented).

3.5.3. Ambient Air Evaporator Governing Equations

As was stated previously, the ambient air evaporator makes use of the condensation to enable higher evaporating temperatures and therefore higher vapor compression cycle COPs. By assuming that $RH_6 = 100\%$ (since RH_5 is set at 90%), T_6 is calculated iteratively by three coupled equations (Equations 3, 19, and 20). Essentially, the condenser load ($\dot{Q}_{\mathrm{heat,M}}$) is set, the evaporator load depends on the heat pump COP, which depends on T_6 (which is dependent on the energy balance in Equation 20). Thus, three unknowns ($\dot{Q}_{\mathrm{evap,M}}$, T_6, and COP_c) are solved iteratively by the EES software.

$$\dot{Q}_{evap,M} = \dot{m}_{a,ex}(h_5 - h_6 - (\omega_5 - \omega_6)h_w) \tag{19}$$

$$\dot{Q}_{evap,M} = \dot{Q}_{cond,M} - \dot{W}_{cond,M} \tag{20}$$

Having determined T_6, the latent heat ratio on the evaporator can be expressed according to Equation 21.

$$LHR = \frac{\dot{m}_{a,ex}(\omega_5 - \omega_6)h_{fg}}{\dot{Q}_{evap,M}} \tag{21}$$

Additionally, the framework can be modified to assess the value of T_6 if no latent heat was available, which can then be used to estimate the heat pump COP when no latent heat is available, as will be shown later.

3.6. Key Performance Metrics

Several performance metrics will be evaluated in this work. The first is the energy savings. The energy savings metric simply compares baseline system power consumption to the MemDry power consumption. The baseline power consumption is simply equal to the vapor compression cycle power consumption. The MemDry total power consumption is given by Equation 22.

$$\dot{W}_M = \dot{W}_{WVC} + \dot{W}_{cond,M} \tag{22}$$

In both systems, fan power consumption is not included in the current models. This would be specific to the system design and is therefore outside the scope of this high-level analysis. Instead, we are more concerned in evaluating the fundamental thermodynamic requirements of heating and dehumidification in the two systems. Next, the drying efficiency relates the latent heat removal rate of the drying process divided by the total system power input, represented generally by Equation 23 [2], [29].

$$\eta_d = \frac{\dot{m}_a(\omega_3 - \omega_1)h_{fg}}{\dot{W}_{sys}} \tag{23}$$

Here, $\dot{W}_{\mathrm{sys}}$ generically represents the total system power consumption for either system (either $\dot{W}_{\mathrm{b}}$ or $\dot{W}_{\mathrm{M}}$). The drying time (t_{dry}) represents the time to remove all of the water from a product. The mass of water in the product to be dried ($m_{\mathrm{w,p}}$) can be set arbitrarily, and then for a given dry time and drying conditions, the air flowrate ($\dot{m}_{\mathrm{a}}$) can be calculated iteratively by the model.

$$t_{dry} = \frac{m_{w,p}}{\dot{m}_a(\omega_1 - \omega_3)} \tag{24}$$

In the analyses of this work, $\dot{m}_{\mathrm{a}}$ is set at 0.0646 kg/s and $m_{\mathrm{w,p}}$ is set at 2.05 kg based on typical clothes drying applications [2]. Of course, the eventual application for this technology is focused on industrial drying, through these clothes drying conditions provide a test case to study the thermodynamics.

4. Results and Discussion

The following results explore the thermodynamic performance of the MemDry concept and compare it to the baseline heat pump system. As has been alluded to in the prior sections, two sets of results are presented in this section: one for the "ideal" scenario and one for a "practical" scenario. Table 1 summarizes the model inputs for these two scenarios.

Table 1. Summary of the model inputs for the ideal and practical scenarios

Variable/Input	Ideal Scenario	Practical Scenario	Practical Scenario Reference
Pinch vapor pressure difference, $\Delta P_{v,pinch}$	0 [kPa]	0.5 [kPa]	[21]
Compressor isentropic efficiency, η_{WVC}	1 [-]	0.70 [-]	[22]
Heat pump second law efficiency, η_{II}	1 [-]	0.40 [-]	[26], [27]

4.1. Energy Savings Over Baseline System

First, the energy savings of the MemDry system compared to the baseline heat pump drying system are evaluated. Figure 3 displays the energy savings for the ideal scenario, and Figure 4 displays the energy savings for the practical scenario.

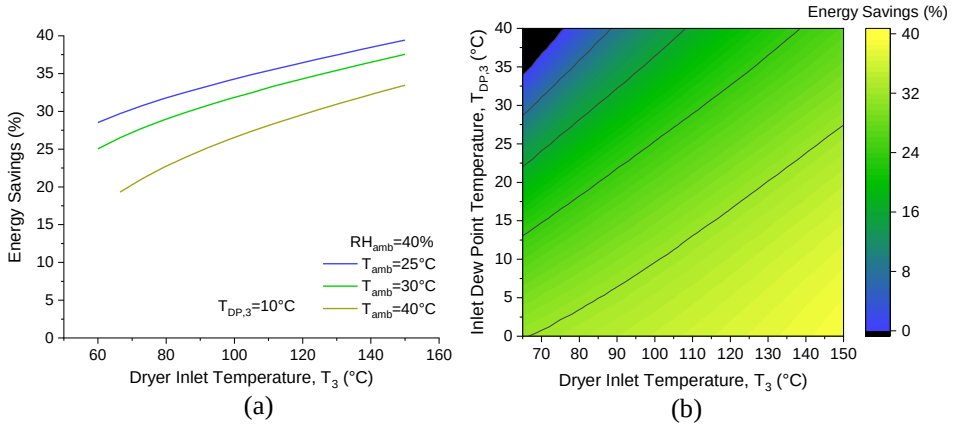

Figure 3. Ideal scenario energy savings. (a) Energy savings of the MemDry system as a function of the drying temperature (T_3) for different ambient temperatures. (b) Energy savings of the MemDry system as a function of the drying temperature (T_3) and dryer inlet dew point temperature ($T_{DP,2}$) for an ambient condition of 30℃ and 40% relative humidity.

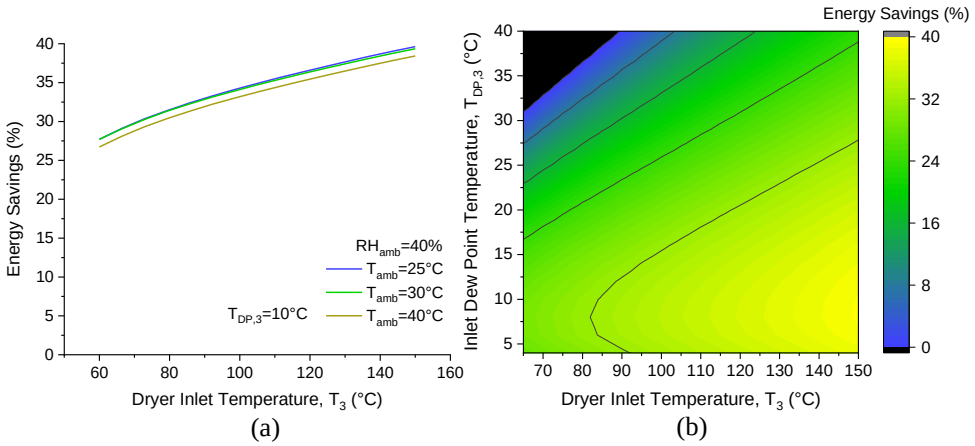

Figure 4. Practical scenario energy savings. (a) Energy savings of the MemDry system as a function of the drying temperature (T_3) for different ambient temperatures. (b) Energy savings of the MemDry system as a function of the drying temperature (T_3) and dryer inlet dew point temperature ($T_{DP,2}$) for an ambient condition of 30℃ and 40% relative humidity.

A few interesting trends can be noticed from these plots. First is that energy savings are generally higher for drying applications with high drying temperatures. As drying temperature increases, the dehumidification load increases exponentially, and reheating energy requirements increase linearly. Since membrane dehumidification specifically targets improving the energy input associated with the humidity loads, it is expected that greater energy savings would be achieved when these humidity loads become more significant. Also, as the ambient humidity ratio increases (increasing temperature at constant relative humidity) the energy savings decrease because the water vapor compressor must pressurize the water vapor to a higher pressure in order to reject it, thus requiring more power input.

In Figure 3a and Figure 4a, it appears as though the "ideal" MemDry system (Figure 3) achieves less energy savings than the "practical" MemDry system (Figure 4) in some conditions, however this is only

because the ideal MemDry system is compared against an ideal baseline system in Figure 3a (both with 100% Carnot efficiency). When practical operating conditions are imposed in Figure 4, the MemDry system does achieve higher savings relative to the baseline system than it did under the ideal operating scenario in Figure 3a because the membrane dehumidification helps alleviate the practical inefficiencies associated with condensation dehumidification in the baseline system that are less pronounced under ideal conditions.

Additionally, for a given drying temperature, an optimal dryer inlet dew point temperature (for the practical scenario) will exist, shown by Figure 4b. At sufficiently low inlet dew point temperatures, very low vacuum pressures are required to achieve this inlet dew point, and therefore the MemDry system achieves lower energy savings. Furthermore, at high inlet dew point temperatures, vapor compression cycles will have a high COP, and therefore the energy savings of membrane dehumidification become less pronounced.

Lastly, the MemDry is not suitable for low-temperature applications with high dryer inlet dew point temperatures (shown by the negative energy savings in the top left of Figure 3b and Figure 4b). In these scenarios, humidity loads would be relatively small and heat pump COPs would be very high, negating the need for energy efficient membrane dehumidification. However, these conditions are not conducive for convective drying and are therefore not likely to be used in many applications.

4.2. MemDry Evaporator Enhancement from Condensation

Next, the enhancement from air-side condensation in the MemDry evaporator is quantified. To clarify this concept, a certain amount of heat must be absorbed by the evaporator to sufficiently reheat the air in the condenser. Without condensation from State 5 to State 6, the evaporator would need to impose a large temperature change to the exhaust air stream. This in turn would mean that lower evaporator temperatures would be required, lowering the heat pump COP. But, with a substantial amount of the evaporator heat being pulled from the condensation process, less temperature change (sensible cooling) is provided to the exhaust air. Therefore, higher evaporator temperatures and higher COPs can be achieved when latent heat is available. The COP assuming no latent heat is available is denoted as COP_{dry}, whereas the COP with available latent heat is denoted COP_{wet} in this section.

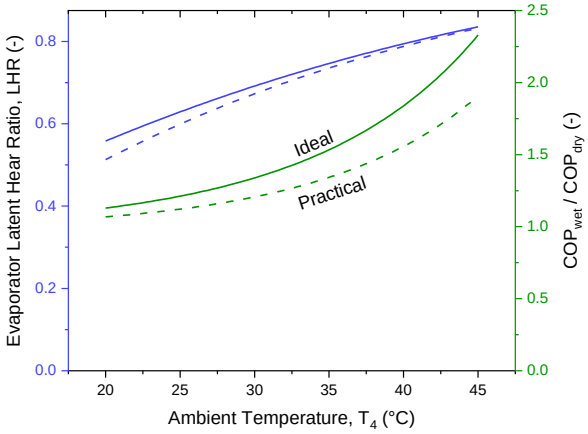

Figure 5. Evaporator latent heat fraction (left axis) and heat pump COP improvement ratio (right axis) as a function of the ambient air temperature for both ideal and practical scenarios. $T_3 = 100℃$ and $T_{DP,3} = 10℃$. Ambient humidity was constant at 40% RH.

For the conditions analyzed in Figure 5, we showed that the latent heat fraction ranged between 0.5 to 0.8. As the LHR increased and the evaporator temperature increased, the heat pump COP could be nearly doubled. Compounding this improved heat pump COP with the lower heating loads and efficient membrane dehumidification, the MemDry concept has great potential to provide significant savings.

4.3. MemDry System Drying Efficiency

Next, we evaluate the drying efficiency, defined by Equation 23, in Figure 6. The drying efficiency is evaluated as function of the drying temperature and inlet dew point temperature for a set ambient condition. As can be seen in Figure 6, the ideal drying efficiency ranges between 3-10 whereas in the practical scenario, the drying efficiency ranges between 0.8-3. A drying efficiency greater than 1 implies that the specific energy input for drying was less than the enthalpy of vaporization for water. A drying efficiency of 1 should be considered the minimum acceptable efficiency. The range of drying efficiencies below 1 in Figure 6a occur

where the heat pump supply temperature is very high (high heat pump energy input and low heat pump COP) and the inlet dew point temperature is low (requiring significant energy consumption from the water vapor compressor). This represents a rather extreme application/condition, though it is important to recall that, even though the drying efficiency dips below 1, the energy savings would still be positive relative the baseline system. Some combination of heat pump heating and resistive heating could potentially bring this drying efficiency closer to 1. Additionally, for a constant dryer temperature, higher inlet dew point temperatures yield a higher drying efficiency, but the drying time will also increase since the air cannot remove as much humidity due to the higher inlet air humidity. Drying time is considered in the next section.

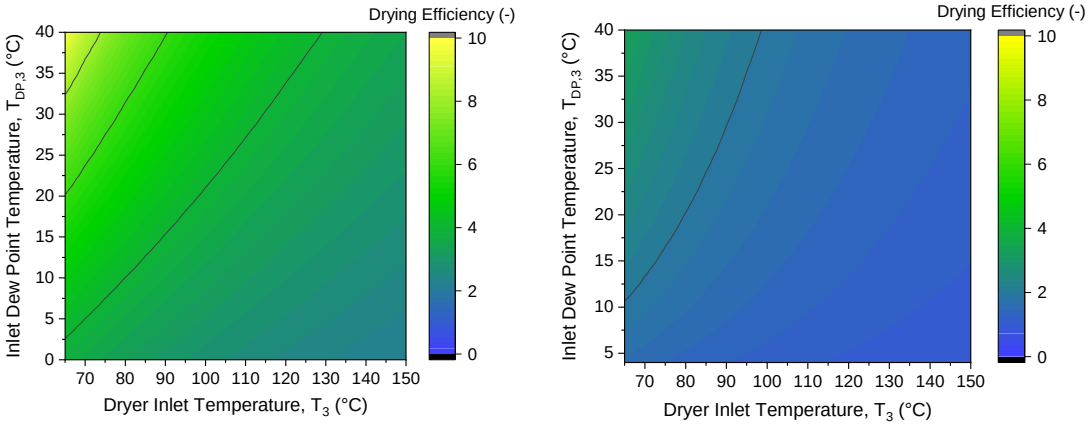

Figure 6. MemDry drying efficiency at the ambient conditions of 30℃ and 40% relative humidity. (a) Drying efficiency in the ideal scenario (b) Drying efficiency in the practical scenario.

4.4. Drying Temperature Reduction

Lastly, we evaluate the impact that the dryer inlet dew point temperature has on the required inlet dryer temperature. The inlet dryer temperature (T_3) is plotted as a function of the dryer inlet dew point temperature for a constant drying time in Figure 7. Essentially, as the inlet to the dryer becomes more humid (higher dew point temperature), a higher drying temperature (T_3) is required to compensate and maintain a constant drying time.

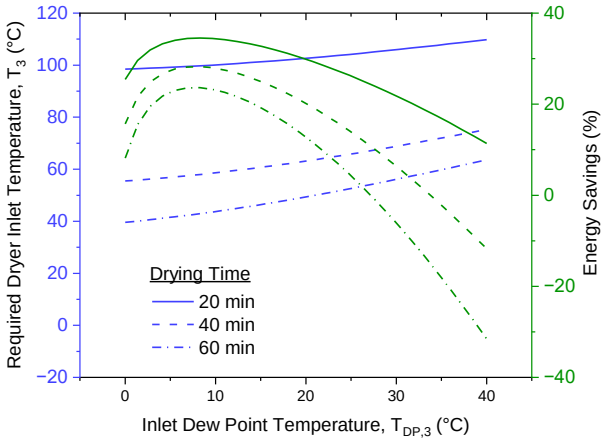

Figure 7. Required drying temperature as a function of the dryer inlet dew point temperature ($T_{DP,3}$) for different constant drying times for the ambient conditions of 30℃ and 40% relative humidity. The energy savings are plotted on the right axis.

As can be seen, reducing the dryer inlet dew point temperature could lead to drying temperature reductions on the order of 10-20℃. This is important for the technology because, achieving exceptionally high temperatures for drying with heat pumps can be challenging. However, if the goal is to electrify many drying processes, reducing inlet humidity conditions with membrane dehumidification can enable lower dryer temperatures (attainable with heat pumps) without sacrificing drying time. Plus, compared to the baseline heat pump system providing the same supply and dew point conditions, the MemDry system may provide energy savings on the order of 20-25% for lower inlet dew point temperature conditions.

5. Conclusions

In conclusion, this work has presented a novel system concept, termed the MemDry system, that combines selective membrane dehumidification with a heat pump for industrial drying applications. The theoretical models were used to explore energy savings and efficiency trends, relative to a baseline heat pump drying system modeled under an identical set of assumptions for fair comparison. It was found that, for the conditions analyzed, up to 40% energy savings could be possible, and negative energy savings are also possible under some extreme conditions. The vapor compression cycle COP can be improved by almost 2x due to the available latent heat in the evaporator for the MemDry, marking a unique advantage to the clever thermal system design. The drying efficiency was found to range between 3-10 under ideal conditions and 0.8-3 under more practical conditions. Furthermore, drying temperatures could be reduced by 10-20℃ while maintaining equivalent drying times and saving up to 25% of the energy input for drying. Overall, the concept shows great potential to offer significant energy savings and process control for industrial drying applications. Future work will focus on prototype development, detailed model development, and detailed model validation.

Nomenclature

Variables and Acronyms

Variable/Acronym Name	Symbol/Abbreviation	Units
Coefficient of Performance	COP	-
Compressor Isentropic Efficiency	η_{WVC}	-
Drying Time	t_{dry}	s
Drying Efficiency	η_{d}	-
Engineering Equation Solver	EES	
Enthalpy	h	kJ/kg
Gas Permeance Units	GPU	-
Humidity Ratio	ω	-
Heat Transfer Rate	$\dot{Q}$	kW
Latent Heat Ratio	LHR	-
Mass Flowrate	$\dot{m}$	kg/s
Mass of Water in Product	$m_{\mathrm{w,p}}$	kg
Power Consumption	$\dot{W}$	kW
Pressure	P	kPa
Pressure Difference	ΔP	kPa
Relative Humidity	RH	%
Second Law Efficiency	η_{II}	-
Temperature	T	℃

Subscripts

Subscript Meaning	Symbol
Air flow	a
Auxiliary Condenser	aux
Ambient Conditions (state 4)	amb
Ambient Exhaust Airflow	ex
Baseline system	b
Condenser	cond
Carnot Heat Pump	Carnot
Cooling	C
Evaporator	evap
Heat of Vaporization	fg
Heating	H
Liquid Water Property	w
MemDry System	M
Pinch Point Difference	pinch
Reheating Requirement	heat
Total System Energy	sys
Water Vapor Property	v
Water Vapor Compressor	WVC

Acknowledgements

We would like to thank Professor Davide Ziviani, Jinwoo Oh and Anand Balaraman for their review and suggestions for the paper. We thank Dr. Kyle Gluesenkamp for sharing his published models [2] for validating our own models. Furthermore, this work has been partially supported by the Center for High Performance Buildings (grant number CHPB-50) at Purdue University. This material is based upon work supported by the U.S. Department of Energy's Office of Energy Efficiency and Renewable Energy (EERE) under the Advanced Manufacturing Office, award number DE-EE0010199. Upon submitting this work, Andrew Fix is supported by an appointment to the Building Technologies Office (BTO) IBUILD Graduate Research Fellowship administered by the Oak Ridge Institute for Science and Education (ORISE) and managed by Oak Ridge National Laboratory (ORNL) for the U.S. Department of Energy (DOE). ORISE is managed by Oak Ridge Associated Universities (ORAU). All opinions expressed in this paper are the authors' and do not necessarily reflect the policies and views of DOE, EERE, BTO, ORISE, ORAU or ORNL.

References

[1] A. S. Mujumdar and Z. H. Wu, "Thermal Drying Technologies: New Developments and Future R&D Potential," *International Conference on Heat Transfer, Fluid Mechanics, and Thermodynamics*, 2007, doi: 10.1142/9789812771957_0001.

[2] K. R. Gluesenkamp and V. K. Patel, "Carnot Analysis of Heat Pump Drying: Ideal Efficiency and Dry Time," in *Purdue Conferences*, 2022.

[3] DOE, "Manufacturing Energy and Carbon Footprints," *Office of Energy Efficiency & Renewable Energy*, 2018. https://www.energy.gov/eere/amo/manufacturing-energy-and-carbon-footprints-2018-mecs (accessed Apr. 11, 2022).

[4] L. J. Goh, M. Y. Othman, S. Mat, H. Ruslan, and K. Sopian, "Review of heat pump systems for drying application," *Renewable and Sustainable Energy Reviews*, vol. 15, no. 9, pp. 4788–4796, 2011, doi: 10.1016/j.rser.2011.07.072.

[5] N. Colak and A. Hepbasli, "A review of heat-pump drying (HPD): Part 2 - Applications and performance assessments," *Energy Convers Manag*, vol. 50, no. 9, pp. 2187–2199, Sep. 2009, doi: 10.1016/j.enconman.2009.04.037.

[6] Z. Erbay and A. Hepbasli, "Application of conventional and advanced exergy analyses to evaluate the performance of a ground-source heat pump (GSHP) dryer used in food drying," *Energy Convers Manag*, vol. 78, pp. 499–507, Feb. 2014, doi: 10.1016/j.enconman.2013.11.009.

[7] Y. Qiu, M. Li, R. H. E. Hassanien, Y. Wang, X. Luo, and Q. Yu, "Performance and operation mode analysis of a heat recovery and thermal storage solar-assisted heat pump drying system," *Solar Energy*, vol. 137, pp. 225–235, Nov. 2016, doi: 10.1016/j.solener.2016.08.016.

[8] M. I. Fadhel, K. Sopian, W. R. W. Daud, and M. A. Alghoul, "Review on advanced of solar assisted chemical heat pump dryer for agriculture produce," *Renewable and Sustainable Energy Reviews*, vol. 15, no. 2. pp. 1152–1168, Feb. 2011. doi: 10.1016/j.rser.2010.10.007.

[9] J. H. Cheng, W. Yu, X. Cao, L. L. Shao, and C. L. Zhang, "Evaluation of heat pump dryers from the perspective of energy efficiency and operational robustness," *Appl Therm Eng*, vol. 215, Oct. 2022, doi: 10.1016/j.applthermaleng.2022.118995.

[10] J. Woods, "Membrane processes for heating, ventilation, and air conditioning," *Renewable and Sustainable Energy Reviews*, vol. 33, pp. 290–304, 2014, doi: 10.1016/j.rser.2014.01.092.

[11] B. Yang, W. Yuan, F. Gao, and B. Guo, "A review of membrane-based air dehumidification," *Indoor and Built Environment*, vol. 24, pp. 11–26, 2015, doi: 10.1177/1420326X13500294.

[12] A. J. Fix, J. E. Braun, and D. M. Warsinger, "Vapor-selective active membrane energy exchanger with mechanical ventilation and indoor air recirculation," *Appl Energy*, vol. 312, p. 118768, 2022, doi: 10.1016/j.apenergy.2022.118768.

[13] D. E. Claridge *et al.*, "A new approach for drying moist air: The ideal Claridge-Culp-Liu dehumidification process with membrane separation, vacuum compression and sub-atmospheric condensation," *International Journal of Refrigeration*, vol. 101, pp. 211–217, 2019, doi: 10.1016/j.ijrefrig.2019.03.025.

[14] M. Qu, O. Abdelaziz, Z. Gao, and H. Yin, "Isothermal membrane-based air dehumidification: A comprehensive review," *Renewable and Sustainable Energy Reviews*, vol. 82, pp. 4060–4069, 2018, doi: 10.1016/j.rser.2017.10.067.

[15] J. G. Wijmans and R. W. Baker, "The solution-diffusion model: a review," *J Memb Sci*, vol. 107, pp. 1–21, 1995, doi: 10.1016/0376-7388(95)00102-I.

[16] F. H. Akhtar, M. Kumar, and K. V. Peinemann, "Pebax®1657/Graphene oxide composite membranes for improved water vapor separation," *J Memb Sci*, vol. 525, pp. 187–194, 2017, doi: 10.1016/j.memsci.2016.10.045.

[17] T. D. Bui *et al.*, "Effect of hygroscopic materials on water vapor permeation and dehumidification performance of poly(vinyl alcohol) membranes," *J Appl Polym Sci*, vol. 134, p. 44765, 2017, doi: 10.1002/app.44765.

[18] Y. Shin *et al.*, "Graphene oxide membranes with high permeability and selectivity for dehumidification of air," *Carbon N Y*, vol. 106, pp. 164–170, 2016, doi: 10.1016/j.carbon.2016.05.023.

[19] T. Puspasari, F. H. Akhtar, W. Ogieglo, O. Alharbi, and K. V. Peinemann, "High dehumidification performance of amorphous cellulose composite membranes prepared from trimethylsilyl cellulose," *J Mater Chem A Mater*, vol. 6, pp. 9271–9279, 2018, doi: 10.1039/c8ta00350e.

[20] O. Labban, T. Chen, A. F. Ghoniem, J. H. Lienhard, and L. K. Norford, "Next-generation HVAC: Prospects for and limitations of desiccant and membrane-based dehumidification and cooling," *Appl Energy*, vol. 200, pp. 330–346, 2017, doi: 10.1016/j.apenergy.2017.05.051.

[21] H. Lim, S. Choi, Y. Cho, S. Kim, and M. Kim, "Comparative thermodynamic analysis of membrane-based vacuum air dehumidification systems," *Appl Therm Eng*, vol. 179, p. 115676, 2020, doi: 10.1016/j.applthermaleng.2020.115676.

[22] A. J. Fix, J. E. Braun, and D. M. Warsinger, "Vapor-selective active membrane energy exchanger for high efficiency outdoor air treatment," *Appl Energy*, vol. 295, p. 116950, 2021, doi: 10.1016/j.apenergy.2021.116950.

[23] A. J. Fix, J. E. Braun, and D. M. Warsinger, "Vapor-Selective Nanostructured Membrane Heat Exchangers for Cooling and Dehumidification," PCT/US2021/019314, 2021

[24] D. E. Claridge and C. Culp, "Systems and methods for air dehumidification and cooling with membrane vapor rejection," US 8,500,848 B2, 2013

[25] S. Klein, "Engineering Equation Solver," vol. v. 10.643, 2019.

[26] C. Mateu-Royo, C. Arpagaus, A. Mota-Babiloni, J. Navarro-Esbrí, and S. S. Bertsch, "Advanced high temperature heat pump configurations using low GWP refrigerants for industrial waste heat recovery: A comprehensive study," *Energy Convers Manag*, vol. 229, 2021, doi: 10.1016/j.enconman.2020.113752.

[27] G. Kosmadakis, C. Arpagaus, P. Neofytou, and S. Bertsch, "Techno-economic analysis of high-temperature heat pumps with low-global warming potential refrigerants for upgrading waste heat up to 150 °C," *Energy Convers Manag*, vol. 226, p. 113488, 2020, doi: 10.1016/j.enconman.2020.113488.

[28] Y. Cengel and M. Boles, *Thermodynamics: An Engineering Approach*, 5th ed. New York: McGraw Hill, 2006.

[29] K. R. Gluesenkamp, V. K. Patel, and A. M. Momen, "Efficiency limits of evaporative fabric drying methods," *Drying Technology*, vol. 39, no. 1, pp. 104–124, 2021, doi: 10.1080/07373937.2020.1839486.